2 Experimental Procedure and LaVa Source Design

The experiments detailed within this thesis employed 1+1 and 1+1′ resonance enhanced multiphoton ionization (REMPI) to probe Au - rare gas (RG) complexes. These complexes are formed in a supersonic jet expansion *via* the ablation of Au into the path of a pulse of rare gas emanating from a pulsed nozzle source. The gold was ablated within a laser vaporization (LaVa) source fixture that facilitated both collisional cooling of the plasma formed during the ablation process and the effective seeding of the metal into the gas prior to supersonic jet expansion into vacuum.

2.1 Apparatus

A schematic of the experimental setup described in this section is shown in Figure 2.1. A laser vaporization source was developed in-house at Nottingham, as described below, to enable the effective pick up, into a pulse of gas, of Au atoms ablated from a solid Au rod (Goodfellow, 99.95%, 25 mm length, 5 mm diameter) using the second harmonic (532 nm at ~ 6 mJ/pulse) of a neodymium-doped yttrium aluminium garnet (Nd:YAG) laser (Continuum Minilite II).

The LaVa source was connected to the high vacuum side of a pulsed nozzle (Series 9, General valves, 750μm orifice, 10 Hz, opening time ≤ 300 μs). Pulsed gas passes into an entrance channel within the LaVa

source and over the Au rod which is rotated and translated slowly (1 step s^{-1}) by a four-phase stepper motor (Philips, unipolar 7.5° step angle, 12V 5.3W) to ensure that a fresh area of the Au surface was continually ablated. The stepper motor was positioned above the LaVa source on a structure that was supported by rods fixed into a chamber flange; the position of motor and LaVa source could be adjusted horizontally to allow easier alignment of the ablation laser through the laser port. The assembly of the stepper motor and the entry position of the ablation laser is shown in Figure 2.2.

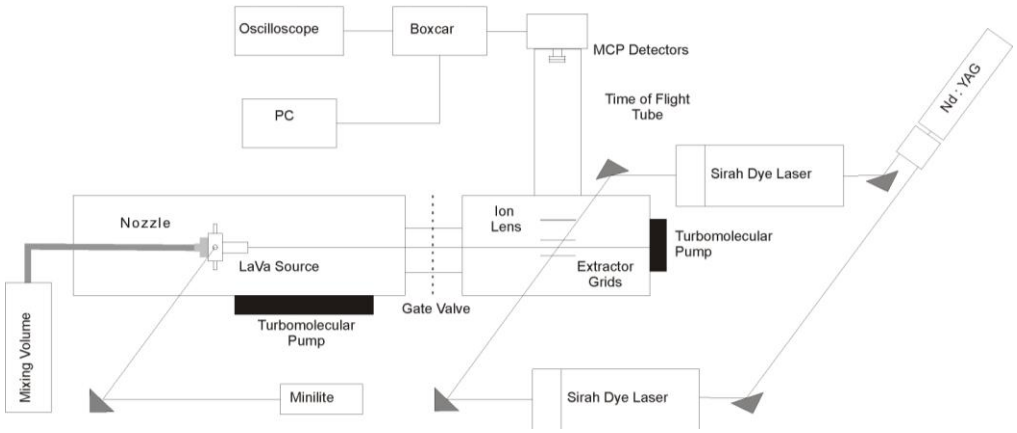

Figure 2.1. Schematic diagram of experimental setup. Diagram adapted from reference 1. The grey triangles represent turning prisms while the dashed line represents the gate valve, which separates the two vacuum chambers. The nozzle chamber is to the left and ionization chamber is to the right.

The gas pulse containing the ablated Au atoms continues through an exit channel, designed as described below to encourage collisional cooling, before exiting the LaVa source and passing into the so-called "nozzle chamber" held at a working pressure of ~ 8×10^{-5} mbar. The timing of the ablating laser pulse was optimized, giving maximum pickup of Au into the gas pulse. Prior to being pulsed into the LaVa source, the gas was held in a mixing volume at a pressure of 2–11 bar;

the gas or mixture of gases was dependent on the complex being studied and will be specified in the experimental section of each individual chapter.

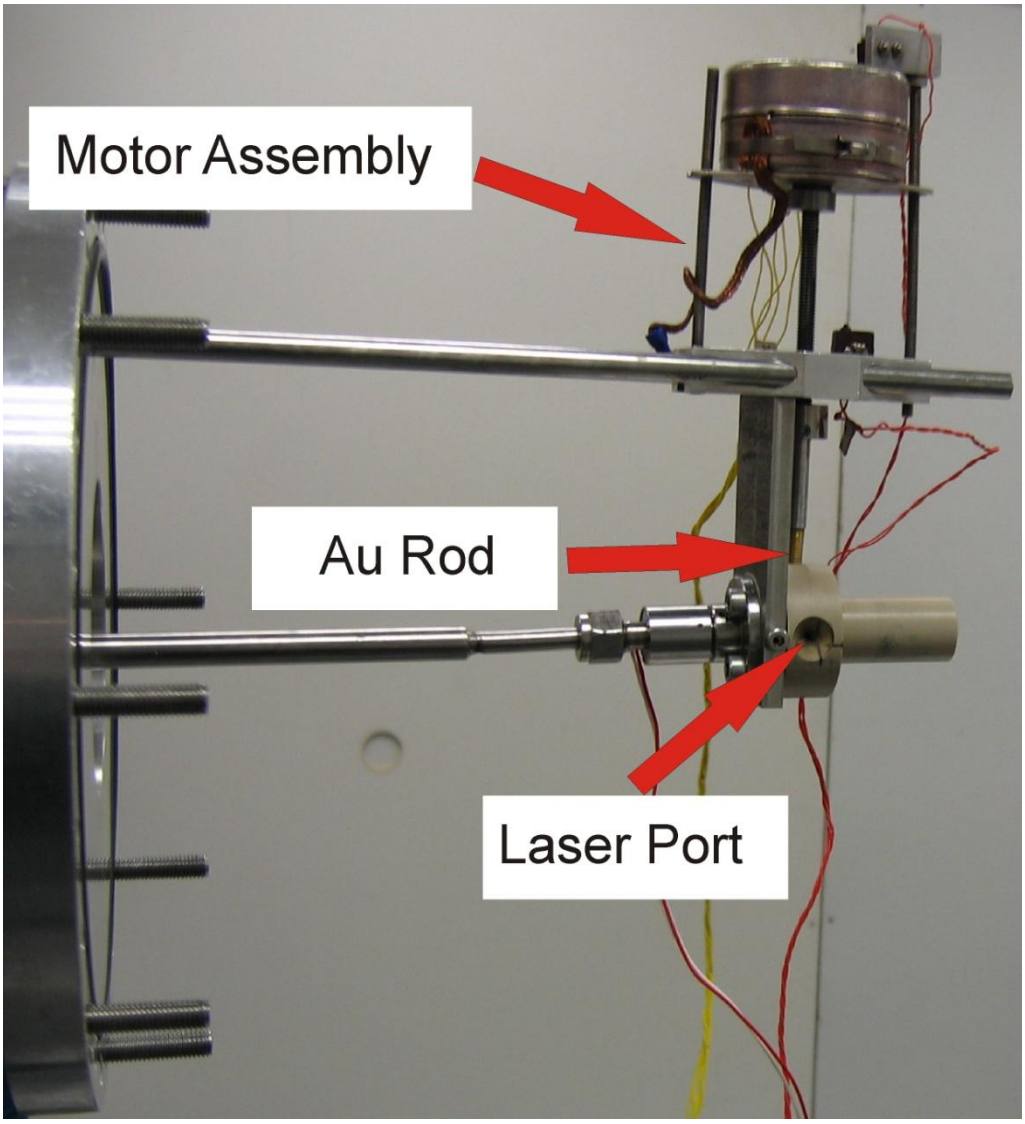

Figure 2.2. Assembly of stepper motor, Au rod, Lava source and Pulsed valve.

On exiting the LaVa source, the pulse of gas seeded with Au atoms enters into the high vacuum region of the nozzle chamber where it forms a supersonic jet expansion (see section 2.3), in which it is expected complex formation will occur. The jet expansion proceeded unskimmed into the extraction region of the ionization chamber, held

at a working pressure of ~ 5 × 10^{-5} bar, where the complexes were probed using REMPI. The ions formed in this process were extracted by a set of charged plates into a time of flight (TOF) tube for detection by a dual microchannel plate (chevron) detector (Photonis imaging sensors). The resulting signal was amplified (SRS SR445A) before being passed to both an oscilloscope (LeCroy LT342 Waverunner) (for monitoring) and a boxcar (SRS SR250) (for integration and averaging). Finally, the signal was then relayed to a computer for storage and analysis, with the initial processing of the data being achieved using the Stanford Research Systems SR272 data acquisition program. The box car was setup to average 10 shots per data point, while the stepsize of the dye laser was set in most cases to be 0.2 cm^{-1}.

Depending on whether a (1+1) or (1+1′) REMPI scheme is being employed, the frequency doubled output (giving a stepsize of 0.4 cm^{-1}) of either one or two tuneable dye lasers (Sirah Cobra Stretch) was used to excite and ionize the complex. The first laser was pumped by the third harmonic (100-150 mJ/pulse at 355 nm, 10Hz) of a Surelite III Nd:YAG laser; the second if required by the second harmonic (100 mJ/pulse at 532 nm, 10Hz) of the same Nd:YAG laser. The nozzle and ionization vacuum chambers were pumped by a 2000 l s^{-1} turbomolecular pump (Pfeiffer TPH 2000), backed by a 40 m^3 h^{-1} rotary pump (Leybold TRIVAC D40B) and 1000 l s^{-1} turbomolecular pump (Leybold TURBOVAC 1000C) backed by a 40 m^3 h^{-1} rotary pump (Leybold TRIVAC D40B) respectively. An additional turbo pump (150 l s^{-1} Leybold TURBOVAC 151) backed by a rotary pump (Leybold TRIVAC D10E) was mounted on the TOF tube. The laser dye used to

produce the required wavelength was specific to the individual experiment and, as with the gas mix, will be specified within each individual chapter.

In order to obtain optimum signal, focusing was found in all cases to be required for the ionization step, hence, for the (1+1) REMPI experiments the output of the dye laser (~ 0.6 mJ pulse^{-1} in the UV) was focussed by a 300mm fused silica focussing lens into the ionization region. In the (1+1′) REMPI experiments the excitation step was performed by the unfocused output, (at a reduced power of ~0.5 mJ pulse^{-1} owing to a reduction in the pump laser power) of the same dye laser; whilst the output of the second dye laser (~0.8 mJ pulse^{-1}), used for the ionization step, was focussed into the ionization region again by a 300mm fused silica focussing lens.

In order to obtain reliable line positions, calibration of the dye lasers was performed. This was carried out by recording spectra of reference Au atomic transitions in the vicinity of the experimental energetic region. These reference transitions were obtained from the NIST physical reference database[7] with the original determination of these line positions being from reference 2. Daily calibration checks were performed, in which the relevant line positions were obtained, at the start of each day in order to confirm the calibration. The linewidth of both dye lasers are expected to be 0.08 cm^{-1}.

The jet expansion, direction of the propagation of the dye laser output, and detection plates were arranged so as to be mutually

perpendicular. The production of the laser pulse was timed so that it would probe the coldest region of the jet expansion where it is expected that the highest concentration of Au-RG complexes will reside. An idea of a general timing scheme is given in Figure 2.3. It should be noted, however, that the timing scheme used in the individual experiments was subject to many conditions (such as the gas used, the pressure the gas was held at in the mixing volume, the position of the pulsed nozzle and also the path length of the lasers which was changed owing to a rearrangement of the lab) and so was optimized for each experimental run.

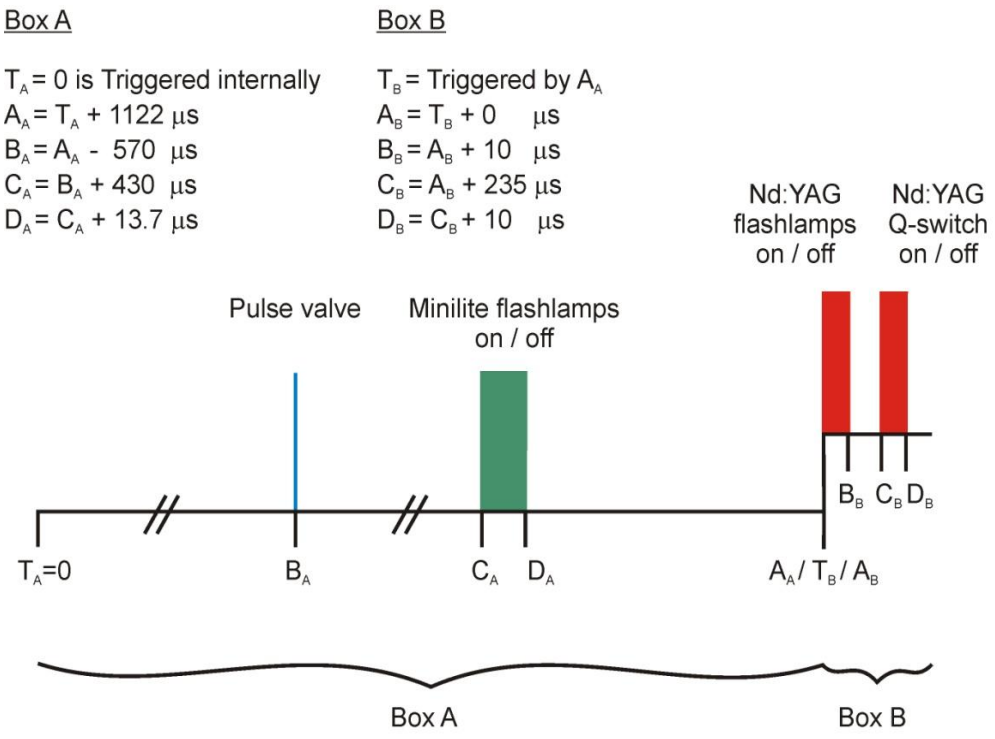

Figure 2.3. Schematic of the general timing scheme used. The internal triggering of the Minilite Q-switch, which was relative to the Minilight flashlamps, is not shown on this timing scheme.

It should be noted that in all cases during the experiments on the Au-RG complexes a number of spectra were recorded in addition to those presented, in which conditions were varied in order to check for effects such as power broadening of the peaks, in which the width of the observed peaks are seen to increase with increasing laser power with no increase in relative intensity of the peak maximum.

2.2 Design of laser vaporization (LaVa) source

A laser vaporization (LaVa) source based on the design by Smalley and co-workers in 1981[3] was developed in-house at Nottingham to enable effective pick up of Au atoms into a pulse of gas. Although the original design of the source was based on previous work, adaptations were made so that the source could be easily used with the apparatus within the Nottingham laboratory; a number of modifications to this original design were made before the final design was settled on.

The designs used by previous groups for laser ablation experiments[3,4,5,6] were considered: in each case their experimental setup was based around a laser vaporization cluster source (LaVa source) attached to a pulsed nozzle source. Despite small differences between the actual designs of the LaVa sources used, on inspection the general principles involved appeared to be similar. The carrier gas employed was directed through a channel flowing over a pure metal or metal-coated rod, at which point ablated metal atoms are seeded into the gas pulse. The seeded gas then flows through a thin channel designed to allow effective mixing of the "hot" ablated metal with the

sample/carrier gas, enabling excess energy in the metal to be dispersed through collisions. The gas then expanded from this channel into a high vacuum region, forming a jet expansion in which clusters are formed. The vaporization of the metal is achieved by the use of a Nd:YAG laser focused by 300mm fused silica focussing lens on to the sample rod.

The original design for the LaVa source attempted to incorporate the general principles discussed above. The LaVa source was connected to the face of the pulsed nozzle, modified to incorporate an "O" ring to ensure a tight seal. The carrier gas was allowed to pass over a rotating, translating sample rod, which was situated in a "waiting room" area of approximate dimensions 6 mm × 12 mm. Three threaded growth channels that could be screwed into the main LaVa source, one of with an internal diameter of 1.5 mm, one of 0.5 mm and one of 0.3 mm were designed in order to allow the effects of the size of the channel aperture to be investigated. The LaVa source and motor were supported by two horizontal metal rods that connected to the rear flange of the chamber. The LaVa source was machined in both brass and polyaryletheretherketone (PEEK) in order to allow testing to determine the most suitable material.

Results of initial testing were promising and a stable source of atomic gold (at the $^2P_{1/2} \leftarrow {}^2S_{1/2}$ resonance of 37358.991 cm^{-1})[7] was quickly found using REMPI, however the formation of complexes was not apparent. A potential problem with our design was that the ablated metal atoms being produced were too "hot" to form clusters. This

problem was avoided by Duncan and co-workers[4] by having a channel that could be extended up to a length of 50mm (~3× longer than our initial design) allowing a longer period for collisional cooling to occur, while Wallimann, Leutwyler and Field[6] physically cooled the actual LaVa source with liquid N_2, finding optimum results at temperatures between -80 and -90°C. Hence, the length of our growth channel was extended and a liquid nitrogen cooling system was developed in which a jacket was machined to allow liquid nitrogen to flow around and effectively cool the Lava source. A schematic of this liquid nitrogen cool system is shown in Figure 2.4, although not shown, the external Dewar was connected to the cooling jacket (that was slipped over the LaVa source) through a pair of flexible bellows. Liquid nitrogen introduced into the top of the externally mounted vacuum insulated Dewar circulated around the LaVa source before exiting out of an outlet located outside of the experimental vacuum chamber. Of the two materials considered for the LaVa source, PEEK was found to be the most suitable owing to the weight of the brass making it more problematic to support the fixture.

Further testing was performed in which the gold signal observed was shown to be independent of the operation of the pulse valve, suggesting that gold was reaching the ionization area whether it was being seeded in the carrier gas or not; furthermore a lot of gas was escaping from the LaVa source in unwanted directions i.e. through the laser ports and rod bore. From this evidence the difficulty in forming complexes could be attributed to the design of the LaVa source not allowing the pulse of gas to flow smoothly through it, as required to

form a supersonic jet expansion. After careful consideration, a relatively major design modification was made and the "waiting room" area feature of Wallimann's design, which was believed to be perturbing the gas flow (reducing the pressure differentional in the LaVa source), was removed and replaced with a straight gas channel. The exit channel size was also reduced to ensure a higher pressure differential of the gas exiting the collisional channel of the LaVa source (high pressure) and entering the vacuum chamber (low pressure); therefore improving the supersonic expansion (see section 2.3). In an attempt to reduce gas loss through the side laser ports, small window/plugs were added, but these proved problematic owing to the large amount of ablated Au being deposited on them. Eventually the windows were replaced with a small countersunk bore hole on the laser side and a small bore hole on the other, which significantly reduced the amount of gas being lost but also allowed easy alignment of the ablation laser.

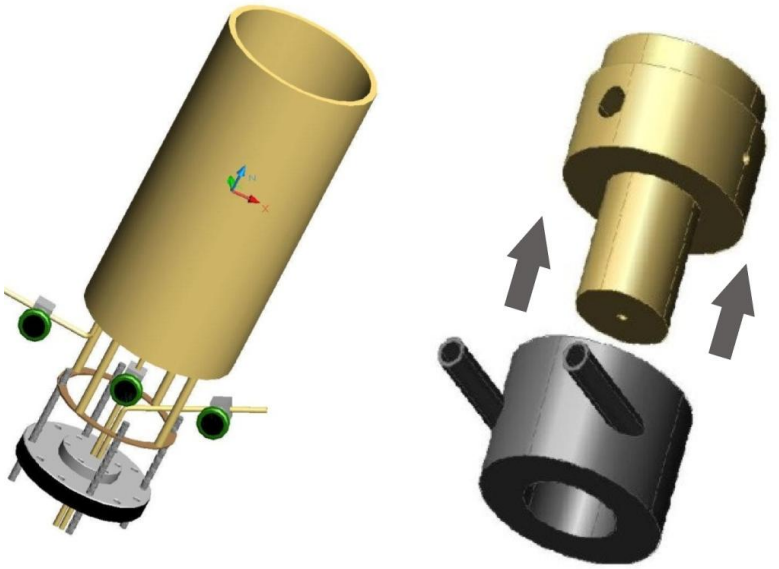

Figure 2.4. Schematic of Liquid nitrogen cooling system.

Subsequent testing was successful and Au–Ar clusters were observed. It appeared that it was the removal of the "waiting room" area that was the critical step in obtaining a functional design although other modifications may also have played a part. With a working system, studies into the effects of small modifications to the design could be performed; the final bore sizes, length of the collisional channel and overall dimensions of the source are shown in Figure 2.5.

Studies into the effectiveness of the liquid nitrogen cooling source proved inconclusive. Owing to convenience and cost issues the majority of experiments were carried out without the liquid nitrogen cooling jacket.

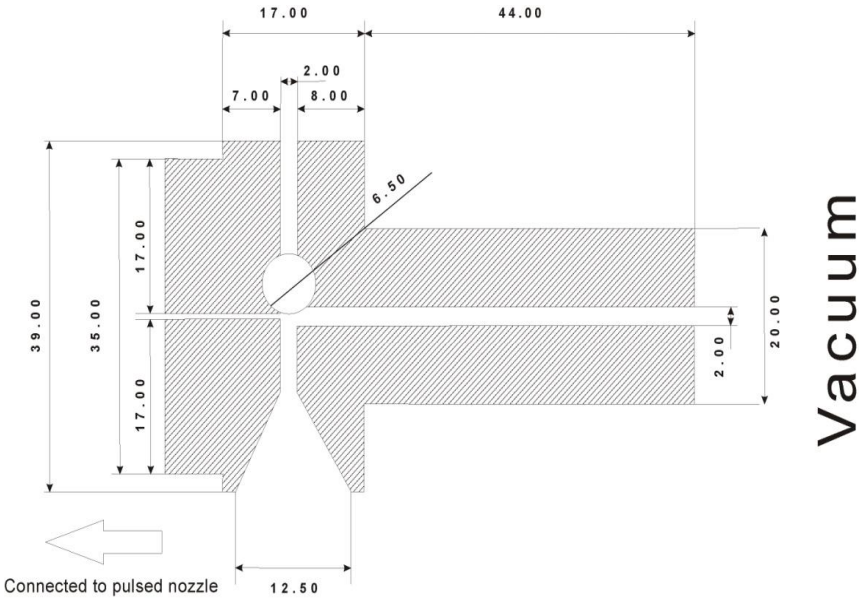

Figure 2.5. Technical diagram of laser vaporization source. Measurements are given in mm.

2.3 Formation of complexes within a supersonic jet expansion

The formation of Au-RG complexes occurs *via* three body collisions within a supersonic jet expansion. An expansion is termed supersonic when its Mach number, defined as;

$$M = {}^{u}/_{a} \qquad (2.1)$$

(where u is the average speed of the gas particles and a is the local speed of sound), is of the order of ~100.[8] If one were to look at the ratio of the average speed of the gas particles in the jet expansion, to the speed of sound at room temperature the Mach number would be modest, however when looking at the ratio when using the speed of sound at the perpendicular translational temperature of the atoms in the jet expansion the Mach number increases dramatically.[9] It is these low temperatures within a supersonic expansion that make it a suitable environment to form weakly bound van der Waals complexes.

In the experiments, gas was held in a mixing volume and pulsed into a vacuum chamber through a small nozzle in the LaVa source of diameter D. The regime of a supersonic jet is where the gas in the mixing volume is at a sufficiently high pressure that $D >> \lambda$ (where λ is the mean free path) resulting in many collisions during passage through into the vacuum chamber. This large number of collisions leads to gas flow with a narrow distribution of velocities (see Figure 2.6), as an atom initially moving rapidly towards the orifice will be slowed down by collisions with slower atoms heading in the same

direction and vice versa. Hence, the atoms within the supersonic expansion may be viewed as having a low translational temperature, whilst the small exit nozzle results in a highly directional gas flow.

The formation of complexes occurs downstream of the nozzle *via* three body collisions in which the excess energy of the collision is removed by the third body i.e.

$$M + Ar + Ar \rightarrow M\text{-}Ar + Ar$$

The probability of a three body collision downstream of the nozzle is, as would be expected, much lower than that of the two body collisions responsible for collisional cooling, and is proportional to $P_r^2 D$, where P_r is the gas pressure in the mixing volume behind the nozzle.[9]

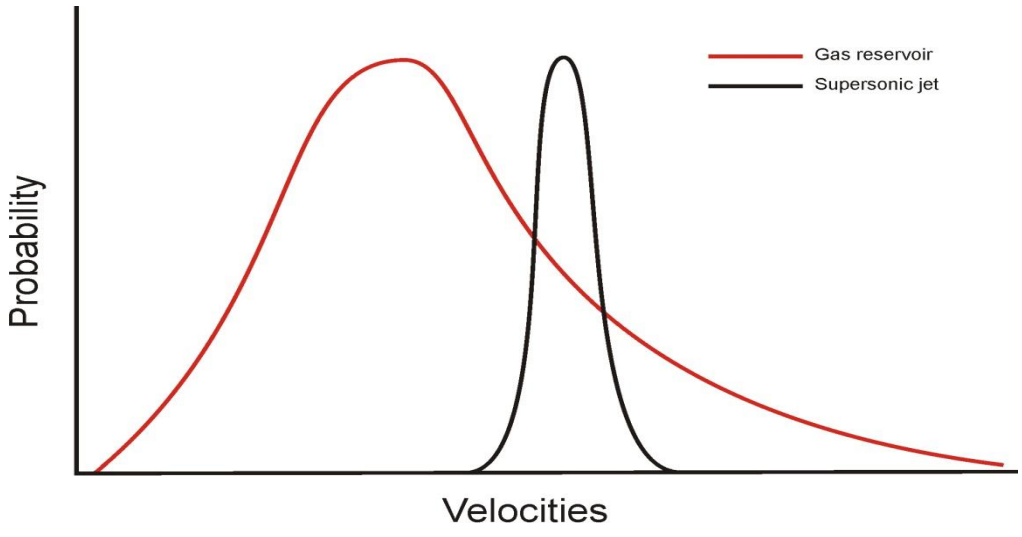

Figure 2.6. Comparison of the range of velocities in the gas reservoir and in the supersonic jet. The supersonic jet can be seen to have a considerably narrower distribution and therefore a considerably lower translational temperature.

An additional benefit of performing spectroscopy within a supersonic expansion is that the complexes produced are internally cold owing to internal energy being converted to translational energy through collisions with the carrier gas atoms. The probability of transfer depends on the magnitude of the energy that is being transferred. The energy difference between adjacent rotational energy levels is considerably smaller than that between adjacent vibrational levels, and it is therefore not surprising that complexes in the expansion are rotationally cooled more efficiently than vibrationally.[9] The advantage of having rotationally cold complexes is that observed peaks are sharper, whilst spectra of vibrationally cooled complexes are less congested with fewer transitions originating from higher vibrational levels in the ground electronic state. However, in some situations, population of the lowest few vibrational states can be an advantage as this allows the energy separation between these occupied levels (in the lower electronic state) to be determined, through the observation of hot bands.

2.4 Resonance enhanced multiphoton ionization (REMPI)

REMPI is a spectroscopic method that allows (ro)vibrational levels in the excited states of complexes to be investigated. Through this method, a number of spectroscopic constants for ground and excited states can be determined. An advantage of using REMPI is that it is sensitive enough to use in experiments where there is a low number density of complexes which is the case in these Au-RG experiments. In most REMPI experiments, and indeed those detailed within this

thesis, the REMPI experiment is coupled with a time-of-flight mass spectrometer (TOF-MS) giving the benefit of mass resolution.

To ionize an atom or a complex, energy is required in order to promote an electron above the specific ionization energy of the atom or molecule; in REMPI this is achieved using a two stage process.[9] In the experiments detailed in this thesis, the first stage is that the complex absorbs a photon to reach an excited electronic state. Whilst the molecule is in this excited state, the absorption of a second photon allows the complex to be ionized. This is called (1+1) or (1+1′) REMPI depending on whether the ionization photon has the same wavelength as the excitation photon or not. Both of these schemes are outlined in Figure 2.7, although it should be noted that other REMPI schemes involving multiple photons for either step are possible. The basic principle of the technique, assuming a two-photon process, is that when the wavelength of the first absorbed photon matches that of a transition between the initial state and that of a higher energy (excited) state, the photon energy is said to be resonant and the chance of the molecule reaching the ionization continuum is greatly enhanced; hence the amount of ions being produced will dramatically increase. In the experiments described herein, the excitation was mainly centred on the Au atom and therefore in the (1+1′) REMPI experiments the second colour was chosen by initial consideration of the energy required to ionize the Au atom from the appropriate atomic state. In fact, the alignment of the laser outputs in the two colour experiments was achieved by the monitoring the Au signal. Once alignment of the lasers on the Au signal was achieved, the ionization

laser could be scanned to find the ionization thresholds for the Au-RG complexes. In these (1+1′) REMPI experiments the ionization laser was fixed at a wavelength above the determined ionization threshold.

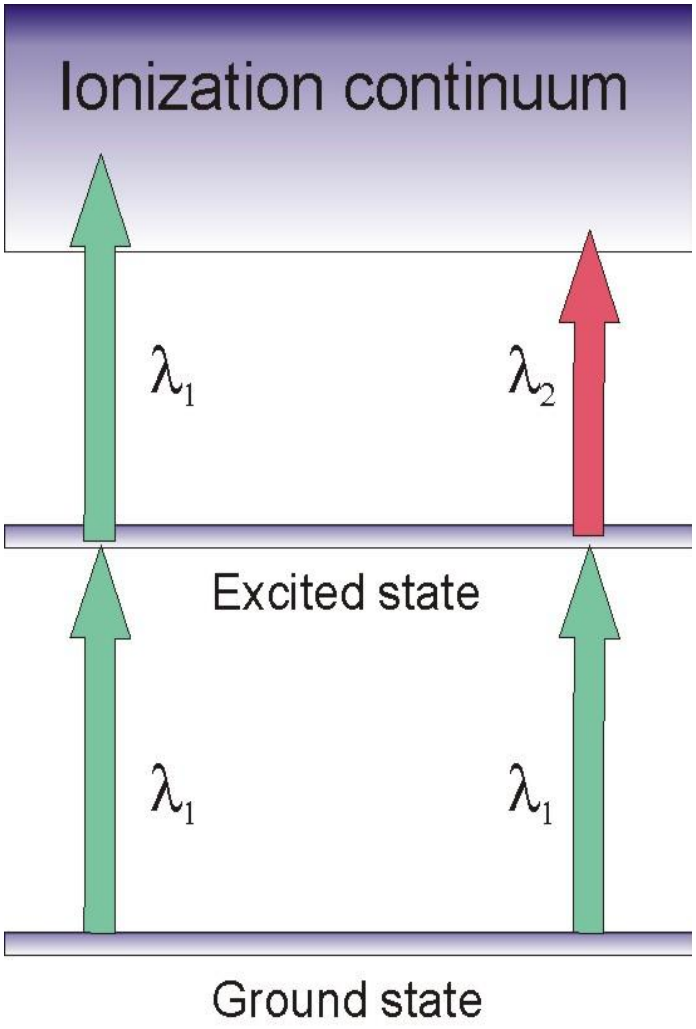

Figure 2.7. Diagram showing the two types of resonance enhanced multiphoton ionization (REMPI). The 1+1' (left) and 1+1 (right) REMPI processes are shown.

In the experiments described, the ions formed in the ionization region by the REMPI process are repelled into a time-of-flight tube where they are detected by microchannel plates (MCPs). The time an ion takes to reach the MCPs depends on the voltages on the repeller plates, the length of the time of flight tube and the mass-to-charge ratio (m/q) of the ion. The voltage on the repeller plates was changed from

experiment to experiment, both to optimize the signal, but also in order to optimize the mass resolution; therefore, the voltages used for the repeller plates is specified in the relevant Chapter for each Au-RG complex. Because of the dependency on mass and charge it is therefore possible in most circumstances to monitor the flux of an individual ion as the laser is scanned across a wavelength range with, as explained above, large increases in signal expected when the laser wavelength is resonant with a transition to a (ro)vibrational level in the excited state.

The REMPI process is dependent on the absorption of photons, in order to promote the molecule to an excited state initially, with the absorption of the second photon resulting in the ionization of the molecule. The probability of the absorption of a photon, however, can differ considerably from molecule to molecule even if the energy separation of the transition in the two molecules is identical. The transition probability can therefore be deduced to be dependent on the specific details of the energy levels involved in the transition. It is these details that give rise to the quantity known as the *transition moment.*[9]

Radiation can only be absorbed if there is an interaction between the molecule and the radiation. Both the electric and magnetic fields present in the electromagnetic radiation may interact with the electric or magnetic fields in a molecule; however, in the context of REMPI spectroscopy it is only the electric fields that are normally important. The intrinsic transition probability is given by $|\boldsymbol{M}_{21}|^2$, where $\boldsymbol{M}_{21}$ is the

transition dipole moment from energy level 1 up to energy level 2. The transition dipole moment is given by equation 2.2

$$\boldsymbol{M}_{21} = \int \psi_2 \boldsymbol{\mu} \psi_1 \, d\tau \qquad (2.2)$$

Where ψ_1 and ψ_2 are the rovibronic wavefunctions of the lower and upper states respectively, and $d\tau$ includes all the relevant coordinates (i.e spatial and spin). The vector quantity $\boldsymbol{\mu}$ is the electric dipole operator.

When a molecule undergoes an electronic transition it is possible that its vibrational and rotational state may also change and therefore also need to be taken into consideration in the determination of the transition probability. The Born-Oppenheimer approximation allows the total wavefunction to be factorized into electronic, vibrational and rotational parts. Ignoring the rotational part of the wavefunction which is only dependent on the nuclear coordinates, owing to the mass of electrons being considerably smaller than that of the nucleus, and separating the dipole moment into electronic and nuclear parts, equation 2.2, written more explicitly in equation 2.3a can be separated to give the transition dipole moment in terms of the electronic and vibrational contributions (equation 2.3b).[10]

$$\boldsymbol{M}_{\text{ev}} = \int \psi_{e'} \psi_{v'} \, (\boldsymbol{\mu}_e + \boldsymbol{\mu}_{\text{N}}) \, \psi_{e''} \psi_{v''} \, d\tau \qquad (2.3a)$$

$$= \int \psi_{e'} \, \boldsymbol{\mu}_e \, \psi_{e''} \, d\tau_{\text{el}} \int \psi_{v'} \, \psi_{v''} \, d\tau_{\text{N}} + \int \psi_{e'} \, \psi_{e''} \, d\tau_{\text{el}} \int \psi_{v'} \, \boldsymbol{\mu}_{\text{N}} \, \psi_{v''} \, d\tau_{\text{N}} \qquad (2.3b)$$

In these equations the subscripts 1 and 2 have been removed and replaced with ′ and ″ to indicate the upper and lower states, respectively. As the electronic wavefunctions of the two different states are orthogonal the second term in equation 2.3b is zero. This gives the dipole moment as

$$\boldsymbol{M}_{\mathrm{ev}} = \mathbf{R}_e \left\langle v' \middle| v'' \right\rangle \tag{2.4}$$

in which

$$\mathbf{R}_e = \int \psi_{e'} \, \boldsymbol{\mu}_e \, \psi_{e''} \, d\tau_{\mathrm{el}} \tag{2.5}$$

is the electronic transition dipole moment, from which it is possible to determine the electronic selection rules. The vibrational overlap integral is given by:

$$\left\langle v' \middle| v'' \right\rangle = \int \psi_{v'} \, \psi_{v''} \, d\tau_{\mathrm{N}} \tag{2.6}$$

the square of which gives the vibrational contribution to the transition probability and is known as the *Franck-Condon Factor* (FCF). The intensity of each vibrational feature of an electronic transition is determined by the population of the initial vibrational level, the intrinsic strength of the transition ($\mathbf{R}_e$) and the FCF. The effect of the FCF on the intensity of vibrational features, and hence the spectrum that would be expected to be observed through REMPI, is shown in

Figure 2.8. In Figure 2.8 the difference between the predicted spectra of two differing states can be seen.

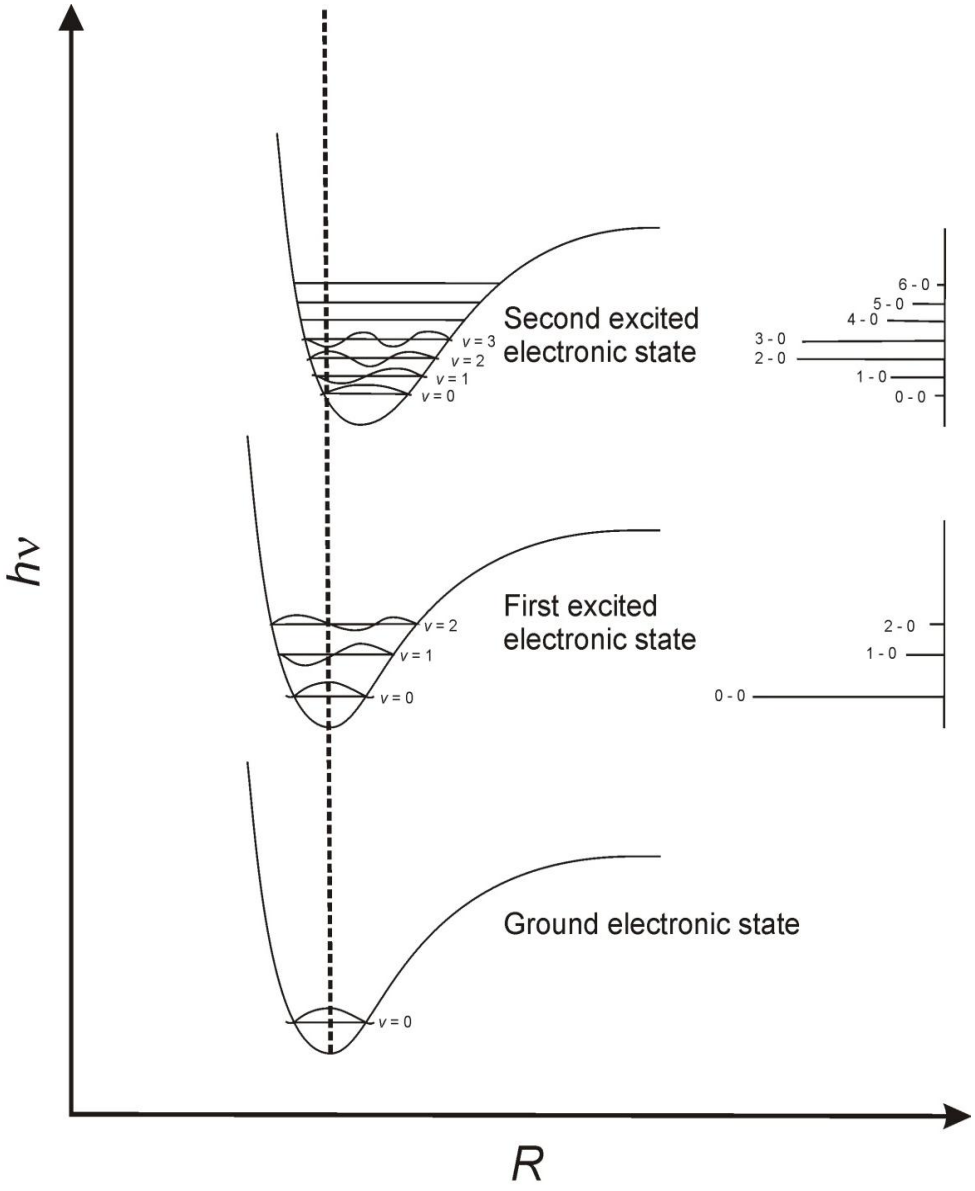

Figure 2.8. Diagram showing how FCF affects the intensity of vibrational bands observed on excitation to an excited electronic state.

There a number of programs that can be used to simulate the expected spectrum of a transition. This is achieved by the determination of the original and final state wavefunctions which can then be substituted into equation 2.5. The wavefunctions of these

states are initially determined through the input of experimentally or computationally derived spectroscopic parameters. The program SpecSim[11] was used to perform the simulations in this work.

As mentioned, the final step in the REMPI processes is the ionization of the complex from the excited state, it is therefore necessary to consider this ionization step and ultimately the fate of ion. The first consideration is whether the complex is being ionized into a bound region of an ion state, in which case considerations of the transition probability, as described above for the initial excitation, have to be taken into account. The second consideration is whether the $[Au\text{-}RG]^+$ ions detected are a result of the ions of other complexes, such as $Au\text{-}RG_2$ or $Au\text{-}RG_3$, dissociating into the $[Au\text{-}RG]^+$ mass channel. Conversely, the possibility that the Au-RG complexes themselves could be dissociating to form Au^+ or even RG^+ also has to be considered. These considerations were taken into account and the associated mass channels were monitored: spectra obtained over a range of powers were also compared as it would be expected any fragmentation would be reduced by attenuation of the laser power.

References

[1] V. L. Ayles, PhD Thesis, *Spectroscopy of small molecules and clusters,* University of Nottingham, 2008.

[2] J. C. Ehrhardt and S. P. Davis, *J. Opt. Soc. Am.*, 1971, **61**, 1342.

[3] T. G. Dietz, M. A. Duncan, D. E. Powers and R. E. Smalley, *J. Chem. Phys.*, 1981, **74** (11), 6511.

[4] K. LaiHing, R. G. Wheeler, W. L. Wilson and M. A. Duncan, (1987) *J. Chem. Phys.*, 1981, **87** (6), 3401.

[5] F. Wallimann, H. M. Frey, S. Leutwyler and M Riley, *Z. Phys. D.*, 1997, **40** (1-4), 30.

[6] F. Wallimann, Dissertation *Laserspektroskopie von Metall-Edelgas-Clustern*, Phil.-nat. Fakultät, Universität Bern, 1997.

[7] http://physics.nist.gov/PhysRefData/Handbook/Tables/goldtable5.htm

[8] J.M. Hollas, *Modern spectroscopy Third Edition*, Jonh Whiley & Sons Ltd., Chichester, 1996.

[9] A. M. Ellis, M. Feher, and T. G. Wright, *Electronic and Photoelectron Spectroscopy Fundamentals and Case Studies*, Cambridge University Press, Cambridge, 2005.

[10] P. F. Bernath, *Spectra of Atoms and Molecules*, Oxford University Press, Oxford, 1995.

[11] SpecSim is a program developed by Kenneth Lawley at the University of Edinburgh.